J Mater Sci (2007) 42:9859–9866
DOI 10.1007/s10853-007-1780-x

Material characterization of blended epoxy resins related to fracture toughness

Andi Haris · Tadaharu Adachi · Yu Hayashi · Wakako Araki

Received: 19 February 2007 / Accepted: 13 April 2007 / Published online: 29 July 2007

Abstract The present study describes the effect of the macromolecular modifications on the fracture toughness of an epoxy system. We synthesized epoxy networks by the reaction of diglycidyl ether of bisphenol A (DGEBA) with methyl-tetrahydro-phthalic anhydride (MTHPA), initiated by a tertiary amine. Several materials were obtained by adding a high molecular weight monomer to one with low molecular weight (both based on DGEBA) at different concentrations. In every case, a stoichiometric amount of MTHPA was employed. The glass transition temperature and the Angell's fragility index, derived from thermo-viscoelastic properties, were used to characterize the materials. Relationship between these two parameters and the fracture properties, including the fracture toughness and the microscopic roughness of the fracture surfaces observed by atomic force microscope (AFM), was then investigated. We found that there were direct correlations among the glass transition temperature, the fragility, the fracture toughness, and the roughness. This study revealed that both the glass transition temperature and the fragility are effective for characterizing material in relation to the fracture toughness of the blended epoxy resins.

Introduction

Among polymeric materials, epoxy resins have been widely used in various engineering fields: structural composites to microelectronics due to their excellent adhesion, chemical resistance, thermal resistance, electrical properties, and mechanical properties. A modified epoxy resin can be developed from blends of simpler epoxy monomers. The epoxy blends are interesting to study for many reasons, including their technological importance (allowing properties to be varied without synthesis of new materials) and the insights that can be gleaned into structure/property relationships [1].

The glass transition temperature and fragility are useful parameters for characterizing cured epoxy resins in relation to their mechanical properties, especially fracture toughness [2–6]. The glass transition temperature is related to the degree of cross-link density [7, 8]. Angell first introduced using the fragility parameter to measure the steepness of viscosity as a function of temperature on approaching the glassy state [9]. The connection between the fragility with other properties of the glass former, such as thermodynamic [10, 11], vibrational [12], and mechanical properties [13, 14], has been the subject of intense research in the recent years [15]. Kanaya et al. [16, 17] reported the relation between the fragility and the dynamical heterogeneity of amorphous polymers. The heterogeneity of amorphous materials was due to ''cooperatively rearranging regions'' as interpreted by Adam and Gibbs [18]. In previous studies, Adachi et al. [2] and Araki et al. [3–5] investigated the relation between the fragility and fracture toughness of epoxy resin and silica particulate-filled epoxy composites with different applied curing conditions. Recently, Kwon and Adachi [6] found that fracture toughness of nano- and micron-silica-particle bidispersed epoxy composites was correlated to the fragility.

In the present study, we investigated the effect of adding a high molecular weight monomer to one with low molecular weight on the fracture toughness of epoxy resin

A. Haris · T. Adachi (✉) · Y. Hayashi · W. Araki
Department of Mechanical Sciences and Engineering, Tokyo Institute of Technology, 2-12-1-I6-1 Ookayama, Meguro-ku, Tokyo 152-8552, Japan
e-mail: adachi@mech.titech.ac.jp

evaluated by the glass transition temperature and the fragility. These two parameters were derived from thermo-viscoelastic properties. Relationship between these two parameters and the fracture properties, including fracture toughness and microscopic roughness of fracture surface observed by atomic force microscope (AFM), was then investigated.

Materials

The materials used in this study were epoxy resins cured from blends of two monomers with different molecular weights. The two monomers were bisphenol A-type epoxide resins: epikote 828 (Japan Epoxy Resins Co. Ltd.) and epikote 1001 (Japan Epoxy Resins Co. Ltd.). Their average molecular weights are 380 and 900, respectively. The weight ratio of epikote 1001 to epikote 828, φ, in the blends ranged from 0 to 30 wt.%. The curing agent and the accelerator were methyl-tetrahydro-phthalic anhydride (MTHPA) (HN-2200R, Hitachi Chemical) and 2,4,6-tris (dimethylaminomethyl) phenol (Daitocurar HD-Acc43, Daito Sangyo), respectively. The curing agent and the blends of the two monomers were mixed in stoichiometric quantities.

Epikote 1001 was dissolved in epikote 828 at 373 K for 70 min and continuously stirred for 10 min. The curing agent and the accelerator were then added to them during another continuous stirring of 10 min at 373 K. Then, the complete mixture was degassed at 373 K in a vacuum oven for 30 min. After this procedure, the mixture was poured in a preheated mold and placed in the oven. The mold, 5 mm × 200 mm × 300 mm, was made of aluminum alloy coated with a Teflon sheet. The curing process for each mixture was carried out at 353 K for 3 h as precuring and at 443 K for 15 h as postcuring. After that, each mixture was allowed to cool slowly in the oven to room temperature. The specimens were machined from the cured plates with a diamond saw to the required dimensions for all tests.

Experimental procedure

Measurement of thermo-viscoelasticity

We used the non-resonance tensile method (with Orientec, Rheovibron DDV-III-EA) for dynamic mechanical analysis (DMA) conducted from 298 to 523 K at frequencies of 2, 6.6, and 20 Hz and a heating rate of 0.5 K/min. The specimens were rectangular bars, 3 mm × 5 mm × 70 mm, and the length between grips was 50 mm. We evaluated the dynamic storage modulus, E', dynamic loss modulus, E'', and damping factor, tan δ, based on the DMA results. The thermal expansion of each specimen was also evaluated from these results.

We determined the glass transition temperature and fragility from the shift factor, a_T, in time-temperature equivalent principle. According to [2, 3], the shift factor, a_T, as a function of temperature is governed by the thermal activation process, and can be expressed as an Arrhenius equation [19]:

$$\ln a_T = \frac{\Delta H}{R}\left(\frac{1}{T} - \frac{1}{T_r}\right), \tag{1}$$

where T, T_r, R, and ΔH are the absolute temperature, the reference temperature, the universal gas constant (= 8.314 J/mol K), and the apparent activation energy, respectively.

The glass transition temperature, T_g, was defined as a temperature at the maximum value of the apparent thermal activation energy as given by the Arrhenius plot of a_T.

Angell [9] defined the fragility, m, as the slope at T_g of the viscosity or the relaxation time in an Arrhenius plot normalized by T_g. Böhmer et al. [20] expressed m as follows:

$$m = \frac{d(\log \tau)}{d(T_g/T)} \quad \text{at} \quad T = T_g, \tag{2}$$

where τ is the relaxation time. Since the epoxy resin has been experimentally known as a thermorheologically simple material [21, 22], a_T is also given as [23]:

$$a_T = \frac{\tau(T)}{\tau(T_r)}. \tag{3}$$

Substituting Eq. (3) into Eq. (2), we can express m as a function of a_T as follows:

$$m = \left.\frac{d(\log\ a_T)}{d(T_g/T)}\right|_{T=T_g} \tag{4}$$

Thus, m can be derived from the slope of a_T with the reciprocal of the temperature normalized by T_g [2–5].

Measurement of mode I fracture toughness

We conducted the mode I fracture toughness tests at room temperature with a universal testing machine (Instron 8501). The specimens were rectangular bars 90 mm long, 20 mm wide, and 5 mm thick. A slot-notch was cut in the specimen with a saw, and a sharp crack was initiated with a razor blade. The slot-notch was 9 mm deep, and the sharp crack was approximately 1 mm deep. The crack length of each specimen was measured by observing fracture surface

with an optical microscope. We performed a standard three-point bending test according to the ASTM-D5045-90, as is shown in Fig. 1. The deflection rate at the loading point was 2.0 μm/s.

Since the load–deformation curve of each specimen was linear until brittle breaking occurred, which means that the stress field near the crack tip was small scale yielding, linear elastic fracture mechanics could be applied to the experimental results to determine the fracture toughness. The critical-stress-intensity factor, K_{IC}, was determined according to the following equations [24]:

$$K_{IC} = \frac{SP_Q}{BW^{3/2}} f(\alpha), \tag{5}$$

where

$$f(\alpha) = \frac{3\alpha^{1/2}\{1.99 - \alpha(1-\alpha)(2.15 - 3.93\alpha + 2.7\alpha^2)\}}{2(1+2\alpha)(1-\alpha)^{3/2}}, \quad \alpha = \frac{a}{W}.$$

Here, P_Q is the maximum load at fracture, and S, B, W, and a are the span length, thickness, width, and crack length of the specimen, respectively. We took the value of facture toughness from the average of at least six data excluding the maximum and minimum ones.

Observation of fracture surface

Visual examination of fracture surfaces was performed using scanning electron microscope (SEM). Approximately, 2 mm thin strips of fractured surfaces with cross sectional area 20 mm × 5 mm were stripped out from the fractured specimens. Fracture surfaces were deposited with a thin layer of gold using a vacuum evaporator.

Quantitative micro-measurements of fracture surfaces were performed with an AFM (Shimadzu SPM-9500J3) operating in tapping mode with lateral scan frequency of 1 Hz. The AFM measurements were performed at room temperature. We analyzed the fracture surfaces from the recorded topography corresponding to changes in amplitude of the oscillating AFM cantilever probe. The scanned area was 3 μm × 3 μm, which is sufficient to determine the microscopic roughness [3]. The location for the AFM scans is described later in section ''Fracture surface''.

We analyzed surface roughness of fracture surfaces by using the three-dimensional roughness height (amplitude) parameter, SR_a, defined as

$$SR_a = \frac{1}{MN}\sum_{m=0}^{M-1}\sum_{n=0}^{N-1}|z(x_m, y_n) - \mu|, \tag{6}$$

where

$$\mu = \frac{1}{MN}\sum_{k=0}^{M-1}\sum_{l=0}^{N-1} z(x_m, y_n).$$

Here, μ is the mean height, M is a number of points per profile, N is the number of profiles, z is the height, and (x, y) are the in-plane cartesian coordinates of the fracture surface.

Results

Thermo-viscoelasticity

Thermo-viscoelastic properties of the cured epoxy resins were characterized in a tensile mode. Figure 2 shows storage moduli, E' and loss moduli, E'' of the epoxy resins at a frequency of 2 Hz. To compare the modulus for each epoxy resin clearly, Fig. 3 plots storage moduli at 298 and 480 K. The storage modulus in the rubbery region decreased with the weight ratio of added epikote 1001, φ,

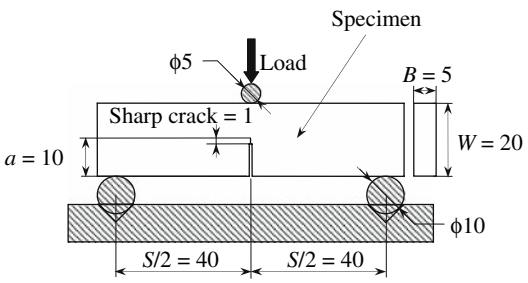

Fig. 1 Three-point bending test. Units in mm

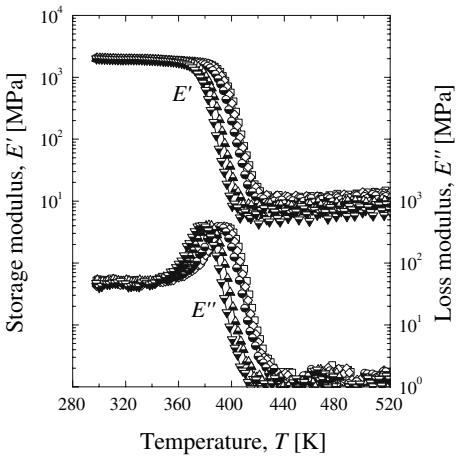

Fig. 2 Temperature dependence of storage modulus and loss modulus at frequency of 2 Hz. Weight ratio of epikote 1001: (□) φ = 0 wt.%; (◇) φ = 5 wt.%; (◒) φ = 10 wt.%; (△) φ = 20 wt.%; (▽) φ = 30 wt.%

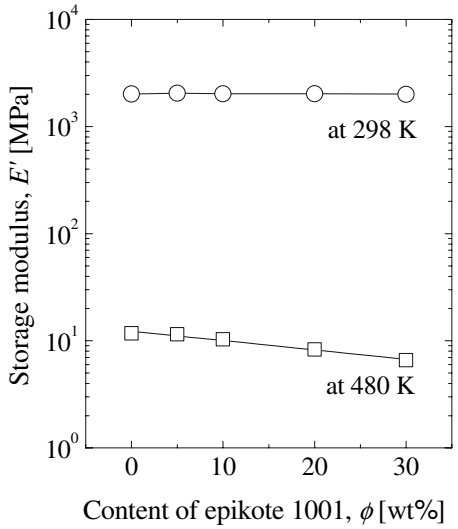

Fig. 3 Storage modulus for weight ratios of epikote 1001

whereas that in the glassy region was approximately constant for φ.

Figure 4 plots linear thermal expansion coefficients of the cured epoxy resins in the glassy region (298–370 K) and rubbery one (405–520 K). We observed the same trend in both glassy and rubbery regions. The linear coefficient of thermal expansion increased slightly with φ.

Glass transition temperature and fragility

By applying the time-temperature equivalent principle [25], we evaluated master curves of storage modulus E' at reference temperature of 298 K from the data at three different frequencies: 2, 6.6, and 20 Hz. The determined shift factor, a_T, for each cured epoxy resin is shown in Fig. 5. Then, these shift factors were used to calculate the glass transition temperature, T_g, and fragility, m.

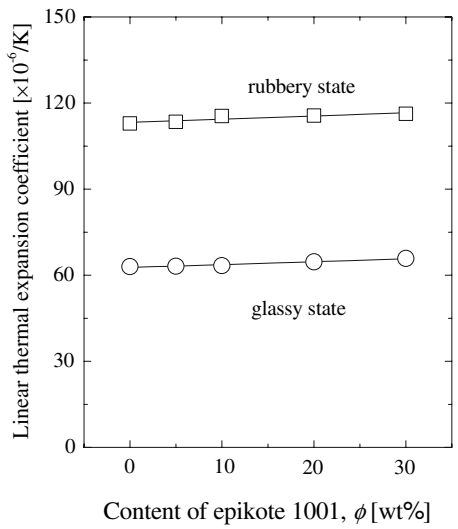

Fig. 4 Linear thermal expansion coefficient

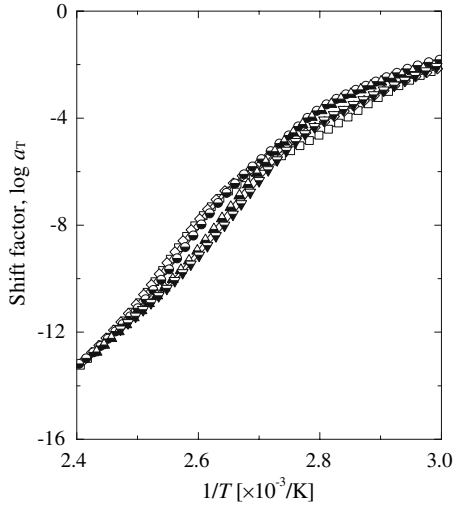

Fig. 5 Shift factor. Reference temperature: 298 K. Weight ratio of epikote 1001: (□) φ = 0 wt.%; (◇) φ = 5 wt.%; (◒) φ = 10 wt.%; (▲) φ = 20 wt.%; (▼) φ = 30 wt.%

The results for T_g are plotted in Fig. 6. The unmodified epikote 828 had a T_g of 391.5 K. The T_g of the epoxy resins decreased with increasing φ. Since T_g expresses the cross-link density of the epoxy resins [7, 8], the epoxy resins with higher φ had lower cross-link densities.

Figure 7 shows the results for m. The value of m decreased from 84.4 to 78.7 as φ increased from 0 to 30 wt.%.

Fracture toughness

Load–displacement curves of the specimens in fracture tests are shown in Fig. 8. The maximum load for the cured

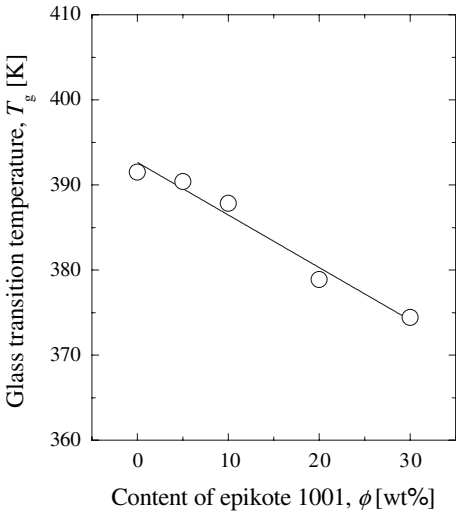

Fig. 6 Glass transition temperature with various weight ratios of epikote 1001

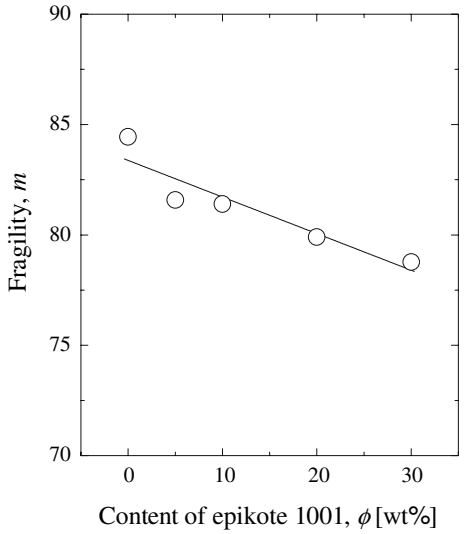

Fig. 7 Fragility with various weight ratios of epikote 1001

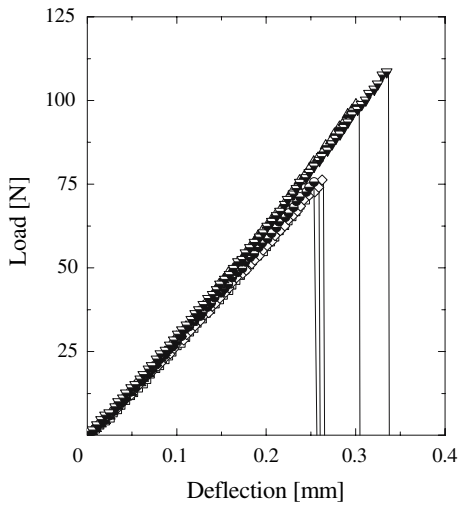

Fig. 8 Load–displacement curves of specimens in fracture test. Weight ratio of epikote 1001: (□) φ = 0 wt.%; (◇) φ = 5 wt.%; (◒) φ = 10 wt.%; (△) φ = 20 wt.%; (▼) φ = 30 wt.%

epoxy resins was approximately constant until φ = 10 wt.%. When φ increased to more than 10 wt.%, the maximum load increased. Since all load–displacement curves were linear until fracture, we could apply linear elastic fracture mechanics to evaluate fracture toughness by using Eq. (5).

Fracture toughnesses, K_{IC}, for specimens with 0–30 wt.% of epikote 1001 are plotted in Fig. 9. Error bars denote the standard deviations of the experimental data. The K_{IC} for the unmodified epikote 828 was 1.06 MPam$^{1/2}$. Below 10 wt.%, adding epikote 1001 provided little or no increase in the K_{IC}. Above 10 wt.%, the K_{IC} grew modestly with epikote 1001 concentration. The K_{IC} of epoxy resin

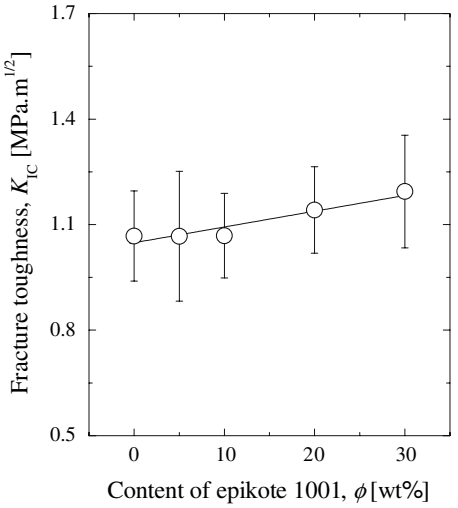

Fig. 9 Fracture toughness with various weight ratios of epikote 1001

with φ = 30 wt.% increased to about 12% more than that of unmodified epikote 828.

Fracture surface

Figure 10 shows schematic and representative fracture surfaces of the cured epoxy resins observed by scanning electron microscope (SEM). As the same as reported by Brown et al. [26], the surface of the fracture plane had striations near the initial crack tip as shown in Fig. 10(b) and (c). Then, the location of scanning area with the AFM was performed in the mirror surface as shown in Fig. 10(a, d, e). The location was approximately 3 mm in front of the initial crack tip of each specimen. The AFM measurements were performed at five different spots which were approximately 500 μm apart from each other within the location. Typical fracture surfaces of unmodified epikote 828 (φ = 0 wt.%) and φ = 30 wt.% are shown in Fig. 11 as the results observed by AFM. The fracture surface of epoxy resin with φ = 30 wt.% was rougher than that of unmodified epikote 828.

The fracture surfaces for all cured epoxy resins were quantified by calculating the surface roughness, SR_a, as defined by Eq. (6). The values of SR_a are shown in Fig. 12. The SR_a increased from 4.9 to 6.9 nm as φ increased from 0 to 30 wt.%.

Discussion

As shown by the results illustrated in Figs. 6 and 7, both the glass transition temperature and the fragility greatly depended on φ and they had the same trend. This means that there is a linear relationship between the fragility and

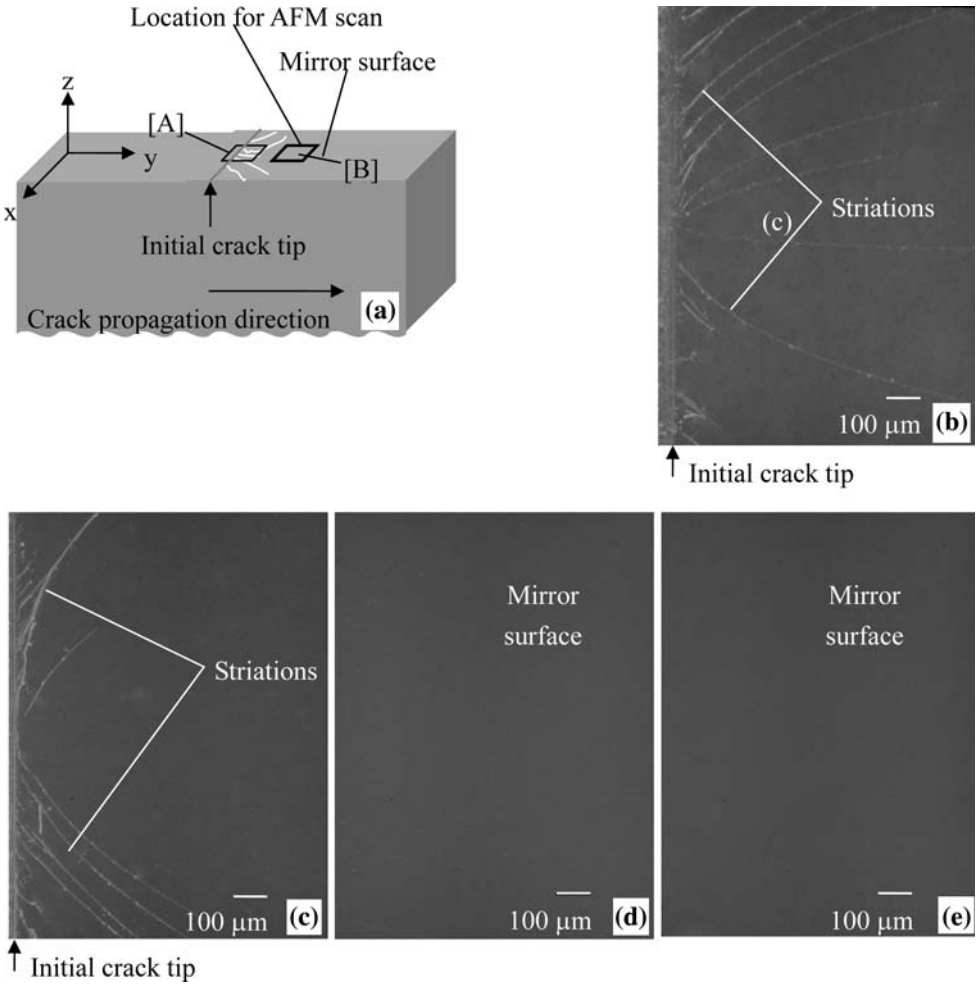

Fig. 10 Schematic and scanning electron micrographs of fracture plane in cured epoxy resins: (**a**) Schematic (not to scale); (**b**) At position [A], with φ = 0 wt.%; (**c**) At position [A], with φ = 30 wt.%; (**d**) At position [B], with φ = 0 wt.%; (**e**) At position [B], with φ = 30 wt.%

the glass transition temperature of the blended epoxy resins. However it should be noted that this may not always be the case because this founding of a positive correlation between the glass transition temperature and the fragility is dissimilar with the results of other works. References [2–6, 27] reported that the fragility is independent of the glass transition temperature of the system.

Figure 13 shows the relationship between the fracture toughness, K_{IC}, and the fragility. Over the range from 0 to 30 wt.% epikote 1001 used in the present work, the K_{IC} increased linearly as the fragility decreased. In other words, the blended epoxy resins with lower fragility index exhibited higher K_{IC}.

Since the glass transition temperature has been correlated linearly with the fragility, the K_{IC} also increased linearly as the glass transition temperature decreased. Specifically, the blended epoxy resin with lower cross-link density had higher K_{IC}. This result is in good agreement with the results of fracture toughness of a series cured epoxy resins from different starting molecular weight monomers reported by Pearson and Yee [28] and Levita et al. [29].

Both the glass transition temperature and the fragility have a clear correlation with the surface roughness, SR_a. For example, we only show the correlation between the fragility and SR_a. When the fragility is plotted against SR_a, as shown in Fig. 14, a strong negative correlation is seen. The fragility decreased linearly from 84.4 to 78.7 as SR_a increased from 4.9 to 6.9 nm.

Conclusion

In this research, we investigated fracture toughness of epoxy resins blended from two monomers with different molecular weights (epikote 828 and epikote 1001) by characterizing the blended resins according to the glass transition temperature and the Angell's fragility index. These two parameters were deduced from thermo-viscoelastic results obtained from DMA.

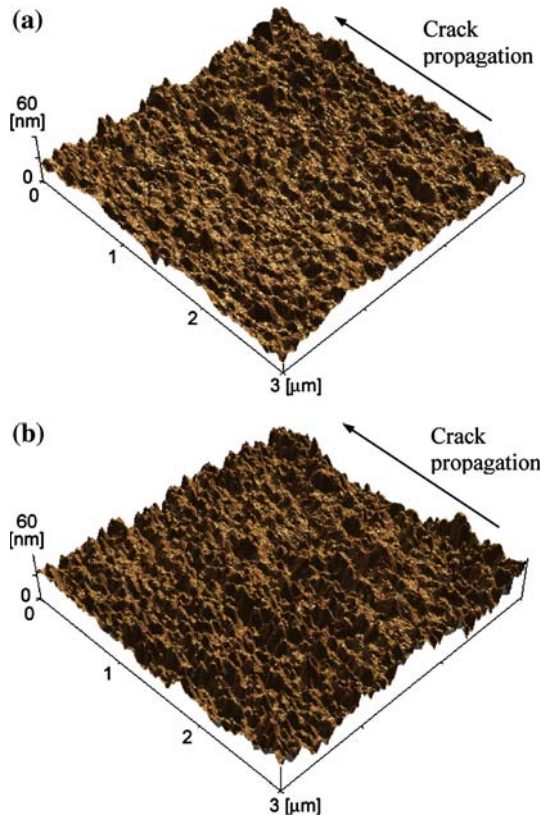

Fig. 11 Fracture surfaces observed by using AFM: (**a**) φ = 0 wt.%; (**b**) φ = 30 wt.%

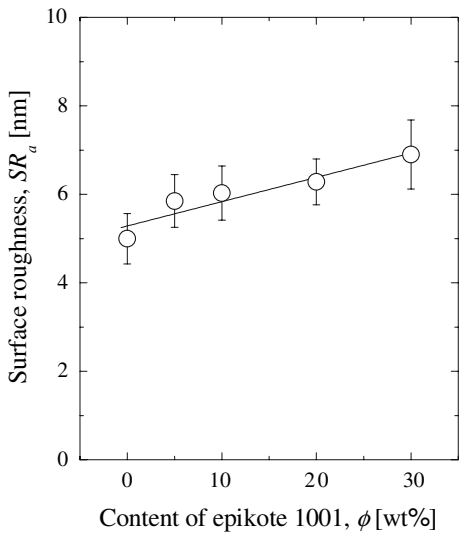

Fig. 12 Surface roughness, SR_a, with various weight ratios of epikote 1001

The experimental results showed that the addition of high molecular weight monomer can improve the fracture toughness of epoxy resin cured from one with low

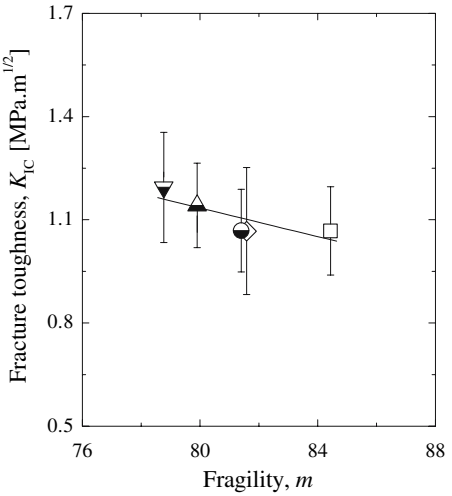

Fig. 13 Relationship between fragility and fracture toughness. Weight ratio of epikote 1001: (□) φ = 0 wt.%; (◇) φ = 5 wt.%; (◒) φ = 10 wt.%; (△) φ = 20 wt.%; (▽) φ = 30 wt.%

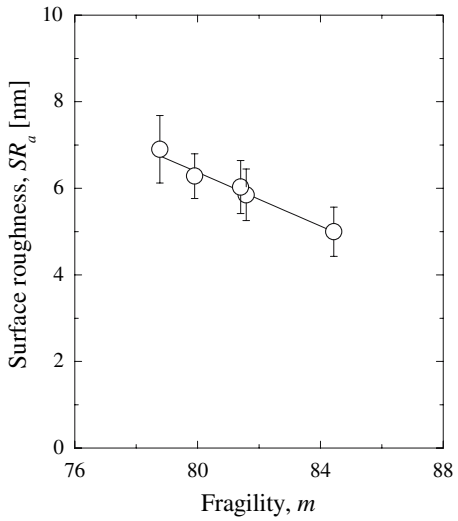

Fig. 14 Relationship between fragility and surface roughness, SR_a

molecular weight without a major reduction of its storage modulus in the glassy state (298 K). Moreover, relationship between the two parameters and the fracture properties, including the fracture toughness and the microscopic roughness of the fracture surfaces observed by AFM, was considered. We found that there were direct correlations among the glass transition temperature, the fragility, the fracture toughness, and the roughness. Our results revealed that both the glass transition temperature and the fragility are effective for characterizing material in relation to the fracture toughness of the blended epoxy resins.

References

1. Roland CM, McGrath KJ, Casalini R (2006) Macromolecules 39:3581
2. Adachi T, Araki W, Nakahara T, Yamaji A, Gamao M (2002) J Appl Polym Sci 86:2261
3. Araki W, Adachi T, Yamaji A, Gamao M (2002) J Appl Polym Sci 86:2266
4. Araki W, Adachi T, Yamaji A (2003) JSME Int J Series A 46:163
5. Araki W, Adachi T, Yamaji A (2006) Rec Res Dev Appl Polym Sci 3:205
6. Kwon SC, Adachi T (2006) J Mater Sci (in press) doi: 10.1007/s10853-006-1025-4
7. Luñak S, Vladyka J, Dušek K (1978) Polymer 19:931
8. Pascault JP, Williams RJJ (1990) J Polym Sci B 28:85
9. Angell CA (1988) J Phys Chem Solid 49:863
10. Ito K, Moynihan CT, Angell CA (1999) Nature (London) 398:492
11. Martinez LM, Angell CA (2001) Nature (London) 410:663
12. Scopigno T, Rocco G, Sette F, Monaco G (2003) Science 302:849
13. Novikov VN, Sokolov AV (2004) Nature (London) 431:961
14. Novikov VN, Sokolov AV, Dyre JC (2004) Nat Mater 3:749
15. Cangialosi D, Alegría A, Colmenero J (2006) J Chem Phys 124:24906
16. Kanaya T, Tsukushi I, Kaji K (1997) Prog Theor Phys Suppl 126:137
17. Kanaya T, Tsukushi I, Kaji K, Gabrys B, Bennington SM (1998) J Non-Cryst Solids 235–237:212
18. Adam G, Gibbs JH (1965) J Chem Phys. 43:139
19. McCrum NG, Read BE, Williams G (1967) Anelastic and dielectric effects in polymeric solids. Wiley, London
20. Böhmer R, Ngai KL, Angell CA, Plazek DJ (1993) J Chem Phys 99:4201
21. Plazek DJ, Choy IC (1989) J Polym Sci B 27:307
22. Plazek DJ, Choy IC, Kelley FN, Meerwall E, Suş LJ (1982) Rubber Chem Technol 56:866
23. Schwarzl F, Staverman AJ (1952) J Appl Phys 23:838
24. Benthem JP, Koiter WT (1975) In: Sih GC (ed) Mechanical fracture, vol 1. Methods of analysis and solutions of crack problems. Noordhoff International Publishing, Leyden, p 155
25. Leaderman H (1943) Elastic and creep properties of filamentous materials and other high polymers. The Textile Foundation, Washington D.C., p 175
26. Brown EN, White SR, Sottos NR (2004) J Mater Sci 39:1703
27. Brüning R, Sutton M (1996) J Non-Cryst Solids 205–207:480
28. Pearson RA, Yee AF (1989) J Mater Sci. 24:2571
29. Levita G, De Petris S, Marchetti A, Lazzeri A (1991) J Mater Sci 26:2348